

PNAS

www.pnas.org

Supplementary Information for

Studies on the mechanism of general anesthesia

Mahmud Arif Pavel, E. Nicholas Petersen, Hao Wang, Richard A. Lerner, and Scott B. Hansen

Paste corresponding author name here

Email: shansen@scripps.edu

This PDF file includes:

Supplementary text
Figures S1 to S6

Supplementary Information Text

Methods

Electrophysiology

Whole cell patch clamp recordings of TREK1 currents were made from TREK-1-transfected HEK 293T cells as described previously(29). Briefly, HEK 293T were cultured in growth media [DMEM, 10% heat-inactivated fetal bovine serum, 1% penicillin/ streptomycin] in a humidified incubator (95% air and 5% CO₂) at 37°C. When the HEK 293T cells were ~90% confluent, they were seed at 50% confluency per 35-mm dish containing 15mm glass coverslips coated with poly-D-lysine (1 mg/ml) to ensure good cell adhesion. The cells were then transiently transfected using X-tremeGENE (Sigma) with a total of 1 µg of DNA per dish. For co-transfection of TREK1, TRAAK with PLD2 or PLD2-K758R cells were transfected with a ratio of 1:3. Human TREK1 pCEH and mouse PLD2 was kindly provided by Dr. Stephen B. Long, Sloan Kettering Institute, NY. TRAAK/Ct-TREK1 (starting at Gly 293) pIRES2eGFP and TREK1/Ct-TRAAK (starting at Gly 255) pIRES2eGFP was kindly provided by Dr. Sandoz Guillaume, iBV CNRS, Université de Nice Sophia Antipolis, France. HEK 293T cells were obtained from ATCC (Manassas, VA). Human TRAAK was a gift from Dr. Steve Brohawn, University of California, Berkeley. Transfected cells were then visualized and selected for electrophysiology 24-48 hours post transfection using green fluorescent protein. Standard whole-cell currents were recorded at room temperature with Axopatch 200B amplifier and Digidata 1440A (Molecular Devices) and measured with Clampex 10.3 (Molecular Devices) at sample rate of 10 kHz and filtered at 2 kHz. The recording micropipettes were made from the borosilicate glass electrode pipettes (B150-86-10, Sutter Instrument) by pulling with the Flaming/Brown micropipette puller (Model P-1000, Sutter instrument). The micropipette resistances were ranged from 3-7 MΩ and filled with the internal solution (in mM): 140 KCl, 3 MgCl₂, 5 EGTA, 10 HEPES, 10 TEA pH 7.4 (adjusted with KOH). The external bath solution contained (in mM): 145 NaCl, 4 KCl, 2 CaCl₂, 1 MgCl₂, 10 HEPES, 10 TEA pH 7.4 (adjusted with NaOH). After the voltage offset was adjusted to zero current between the patch electrode and the bath solution, the whole cell configuration was achieved by repetitive gentle suctions on cells sealed at 1-10 GΩ. In the whole cell configuration, cells were held at -60 mV and currents were elicited by voltage steps command (at -100 to +100 mV from V_{hold} = -60 mV) and voltage ramp commands (-100 mV to +50 mV in 5 ms). Volatile anesthetic, chloroform, was applied using a gravity-driven (5 mL/min) gas-tight perfusion systems (valves and tubing were made of PTFE). HEK 293T cells were perfused with control solution or the test solution that contained the volatile anesthetic. Chloroform was dissolved based on the anesthetic saturation experiments that it has 66.6 mM solubility in water at 37°C(30). Subsequently, data were replayed and analyzed using Clampfit 10 (Molecular Devices) to generate current-voltage relationship (I-V Curve) from voltage steps protocol. Student's *t*-test was applied to assess statistical significance using Prism6 (GraphPad software) and judged significant at *p* < 0.001. The values represented in the graphs are mean ± SEM.

Channel purification and flux assay

TREK-1 channel protein purification and flux assay were done as previously described(35, 36). Briefly, *Pichia* yeast was used to express zebrafish TREK-1 (1-322 amino acids) containing GFP at C-terminus. Followed by cryo milling, the extraction of the proteins was done in dodecyl-β-d-maltoside (DDM) with protease inhibitors. The proteins were then purified on a cobalt affinity column to homogeneity followed by size exclusion chromatography (SEC). The final SEC buffer contained 20 mM Tris (pH 8.0), 150 mM KCl, 1 mM EDTA, and 2 mM DDM. All proteins were collected with a predominant monodispersed peak corresponding to the expected molecular weight (MW) of the assembled channel protein plus GFPs. This purified TREK-1 was used to generate proteoliposomes by mixing 1:100 TREK-1/lipids. The ratio of the lipids (85% DOPC and 15% DOPG) were mixed, dried, and solubilized in rehydration buffer (150 mM KCl, 20 mM HEPES [pH 7.4]) and calibrated with 3 mM DDM before the channel mixing. DDM was then removed by BioBeads (Bio-Rad) and the proteoliposomes (5 µL) were sonicated and added to 195 µL of flux assay buffer (150 mM NaCl, 20 mM HEPES [pH 7.4], 2 µM 9-amino-6-chloro-2-methoxyacridine [ACMA]) in a 96-well plate (Costar 3915) at room temperature. A protocol was set up on a Tecan M200 Pro to initially read the fluorescence (excitation 410, emission 490) every twenty seconds for one minute as a baseline. The temperature inside the plate reader was set at 25°C. Flux was

initiated by the addition of the protonophore carbonyl cyanide m-chlorophenyl hydrazone (CCCP) (3.2 μ M) by collapsing the electrical potential allowing protons into the vesicles. Fluorescence was read every twenty seconds for seven minutes. Next, the potassium-selective ionophore valinomycin (20nM final concentration) was added to terminate the chemical gradient, and fluorescence was read every twenty seconds for five to ten minutes. An average of the duplicates was taken, and then the data was normalized. Briefly, at each time point $(F - F_{start}) / (F_{start} - F_{end})$ was calculated, where F is the fluorescent value at that time, F_{start} is the average of the first four initial readings before the addition of CCCP, and F_{end} is the final fluorescent value after 5 minutes of valinomycin. The control proteoliposome flux was normalized to 1 throughout CCCP, and the TREK flux was normalized to the control accordingly. In flux assay figures, addition of CCCP occurs at $t=80$ seconds and ends at $t=520$ seconds before valinomycin was added.

SDS PAGE and western blot

HEK 293T cells were transiently transfected using X-treme gene 9 (Sigma Aldrich). After 48 hours of the transfection, cells were homogenized in the ice-cold lysis buffer comprising 1.5% DDM (Anatrace), 10% Glycerol (Fisher Scientific), 1 mM EDTA (Sigma), and 1: 100 protease inhibitors (calbiochem) in 1X PBS, pH 7.5. Lysates were centrifuged at 17,000g for an hour at 4°C to collect the supernatant. Protein sample were diluted 1:1 with 2X SDS Laemmle buffer (Bio-Rad) and incubated for 30 mins at 37°C. The denatured proteins were then separated on 4-20% SDS polyacrylamide gel (Mini-PROTEAN® TGX™, Bio-Rad) and blotted onto polyvinylidene difluoride membranes and probed with rabbit monoclonal antibody against PLD2 (E1Y9G, Cell Signaling). Blot signals were visualized with an AlphaImager™ Gel Imaging System (Alpha Innotech).

Fluorescence recovery after photobleaching (FRAP)

For FRAP studies, N2a and C2C12 cells were grown in DMEM with 10% FBS until 16 hours before use in which they were switched into serum free DMEM. On the day of the experiment, DMEM in live cells was replaced with DMEM w/o phenol red. Fixed cells were rinsed once with PBS and then put into a mixture of PBS with 3% PFA and 0.1% glutaraldehyde for 20 min at 37°C. Fixed cells were then rinsed with PBS 5 x 5 min and then placed back into phenol-free DMEM. CTxB (ThermoFisher C34778, 100 μ g/ml) was then applied 1:200 into each plate and allowed to incubate for >30 min before imaging. Imaging and data collection were performed on a Leica SP8 confocal microscope with the Application Suite X v.1.1.0.12420. 5 images were taken as baseline after which a selection of 1 or more ROI was bleached at 100% laser power for 6-8 frames. Recovery was measured out to 5 min and fluorescence of the ROI(s) were quantified. The fluorescence before bleaching was normalized to 1 and after the bleaching step was normalized to 0.

Supplementary Information Figures

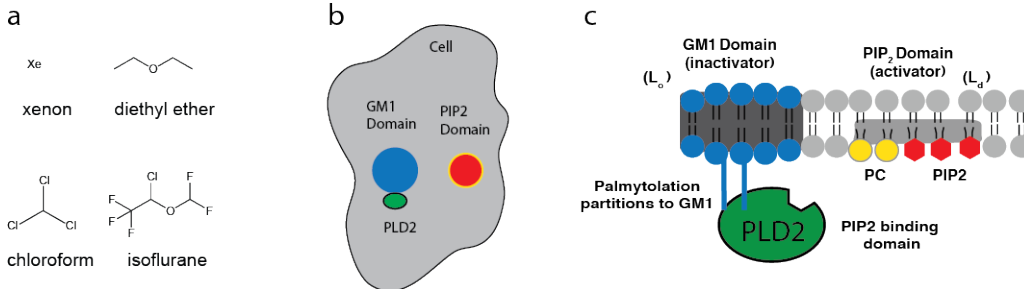


Fig. S1. GM1 rafts and PLD2 activation by substrate presentation. **a**, Chemical structures of select inhaled anesthetics are shown. Diversity ranges from xenon, a single hydrophobic atom, to chloroform, chlorinated carbon, and ether compounds. **b**, the organization of PLD2 and lipid rafts on the surface of a cell are shown (not to scale). GM1 rafts are comprised of GM1 saturated lipids and cholesterol, palmitoylation drives PLD2 into GM1 rafts (blue circle) where it is sequestered away from its substrate polyunsaturated PC and PIP₂ rafts (Red circle with yellow outline). **c**, Side view of the membrane in (b) with PLD2 localized to the inner leaflet through two palmitoylation sites (blue lines). GM1 rafts also commonly referred to as the liquid ordered phase (L_o) are thicker than the liquid disordered phase (L_d). We previously showed mechanical force disrupts lipid rafts and causes PLD2 translocation to PIP₂ rafts. PLD2 has a PIP₂ binding site and resides in equilibrium between GM1 and PIP₂ rafts. PIP₂ is polyunsaturated and preferentially localized with unsaturated PC—PLD2 generates unsaturated PA and PG products through substrate presentation (22).

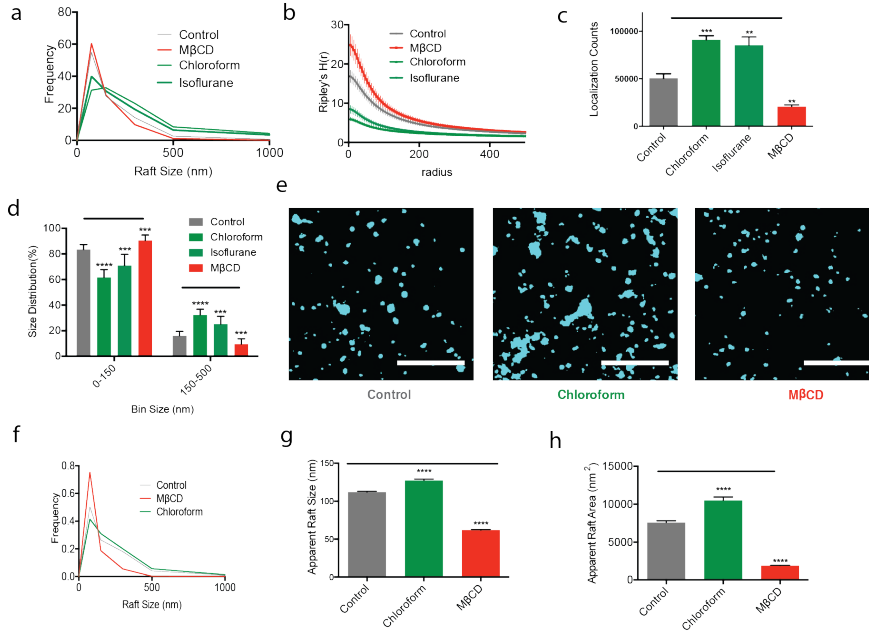


Fig. S2. Inhaled anesthetics disrupt GM1 rafts. **a**, Particle size distribution curve of the lipid rafts in N2A cells after chloroform, isoflurane, and MβCD treatments (n=10). The number of rafts smaller than 150 nm decreased and the rafts larger than 150 nm increased (see panel (d) for quantification). **b**, Derivatives of Ripley's K-Function (H(r)) demonstrating the separation of GM1 rafts with or without treatment of the inhaled anesthetics (1 mM) or MβCD (100 μM) (± s.e.m., n = 10). **c**, Bar graphs showing the amount of particle localizations acquired within the fixed frames numbers (10000) (± s.e.m., n = 5). **d**, Histograms showing the apparent size distribution of lipid rafts from N2A cells in (a) binned from 0-150 nm and 150-500 nm. Chloroform (1mM) and isoflurane (1mM) both shift from small to large and MβCD (100 μM) shifts from large to small (± s.e.m., n = 10). Both observations are a form of disruption. **e**, Representative super-resolution (dSTORM) images of lipid rafts from C2C12 cells before and after the treatment with inhaled anesthetics or MβCD (100 μM) (Scale bars: 1 μm). **f**, Particle size distribution curve of the lipid rafts after the chloroform, isoflurane, and MβCD treatments from multiple C2C12 cells (n = 6-8). **g-h**, Bar graphs comparing the apparent lipid raft sizes (g) and areas (h) quantified by cluster analysis showing the disruption of lipid raft by chloroform and MβCD (± s.e.m., n = 2844-6525). Student's t-test results: ***P<0.001; ****P<0.0001.

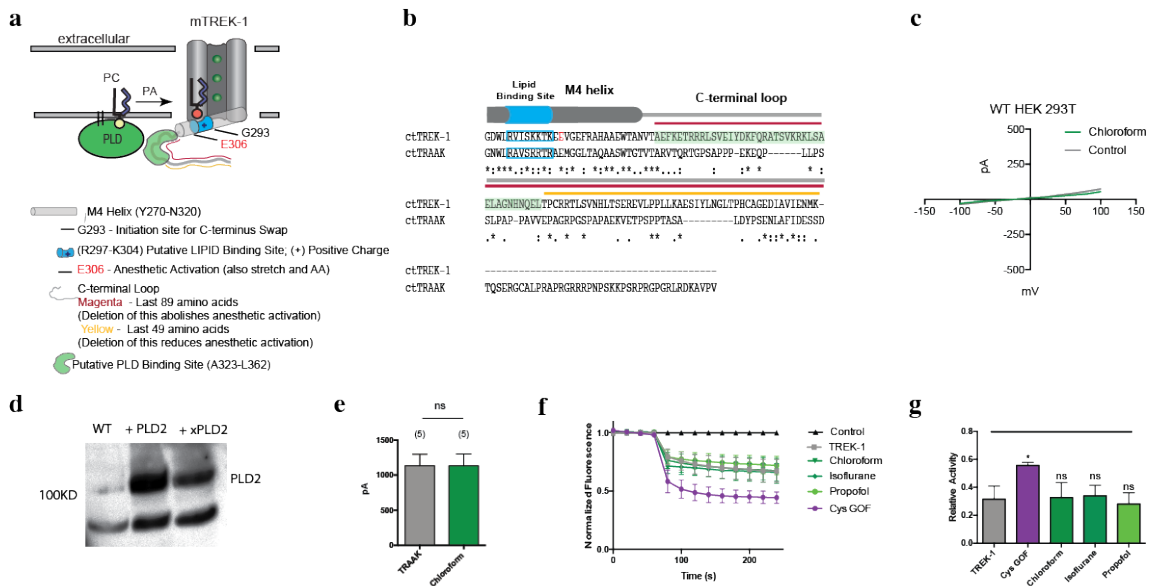


Fig. S3. General anesthetics activate TREK-1 through PLD2. **a**, Cartoon depicting the amino acids that are known to play a role in anesthetic activation and the PLD2 dependent lipid-gating of TREK-1 channels. **b**, Multiple-sequence alignment between the swapped C-terminus of mouse TREK-1 (293-411) and TRAAK (255-398) generated with Clustal Omega (EMBL-EBI). The colors and features correspond with panel (a). **c**, Current-voltage relationship (I-V) for untransfected HEK 293T are shown. No changes in whole-cell currents were observed after treatment with 1 mM of chloroform. **d**, Western blot showing the over expression of wtPLD2, mPLD2 and xPLD2 from transfected HEK 293T cells. **e**, Bar graph summarizing wt. TRAAK channel currents when activated by chloroform (1mM) at +40 mV (\pm s.e.m., $n = 5$) confirming earlier studies that TRAAK is anesthetic insensitive. **f**, Ion flux assay of purified TREK-1 reconstituted into DOPC (16:1) liposomes with 15 mol% DOPG anionic lipid. Anesthetics chloroform (1 mM), isoflurane (1 mM), and propofol (50 μ M) had no significant effect on channel currents compare to the double cysteine gain of function mutation (Cys GOF) (\pm s.e.m., $n = 3-5$). **g**, Bar graph comparing the relative activity from **f**.

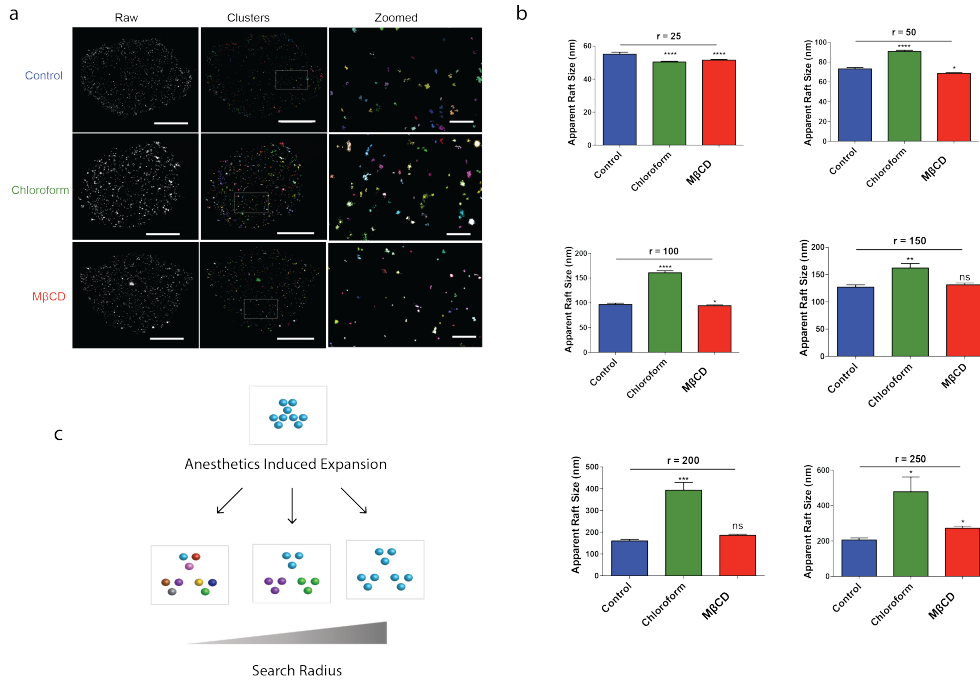


Fig. S4. Effect of search radius on observed raft size. **a**, Representative images showing the raw images with particle localizations (left panel, scale bar = 5 μm), clustered particles (DBSCAN) to determine raft sizes (middle panel, scale bar = 5 μm), and the zoomed in (right panel, scale bar = 0.5 μm) using 100 nm search radius. Arbitrary colors are assigned to particles of the same cluster. **b**, Bar graphs showing the changes in apparent raft sizes after anesthetic treatment at various search radius (ϵ) when at least 10 localizations were clustered. **c**, Cartoon depicting the size variation at different search radius. A radius that is too small will treat each particle as an individual cluster and give cluster that are too small. A search radius that is too large clusters separate molecules giving an artificially large size. The search radius of 100 nm shown in (a) and used for this study shows appropriate clustering and a significant increase in size.

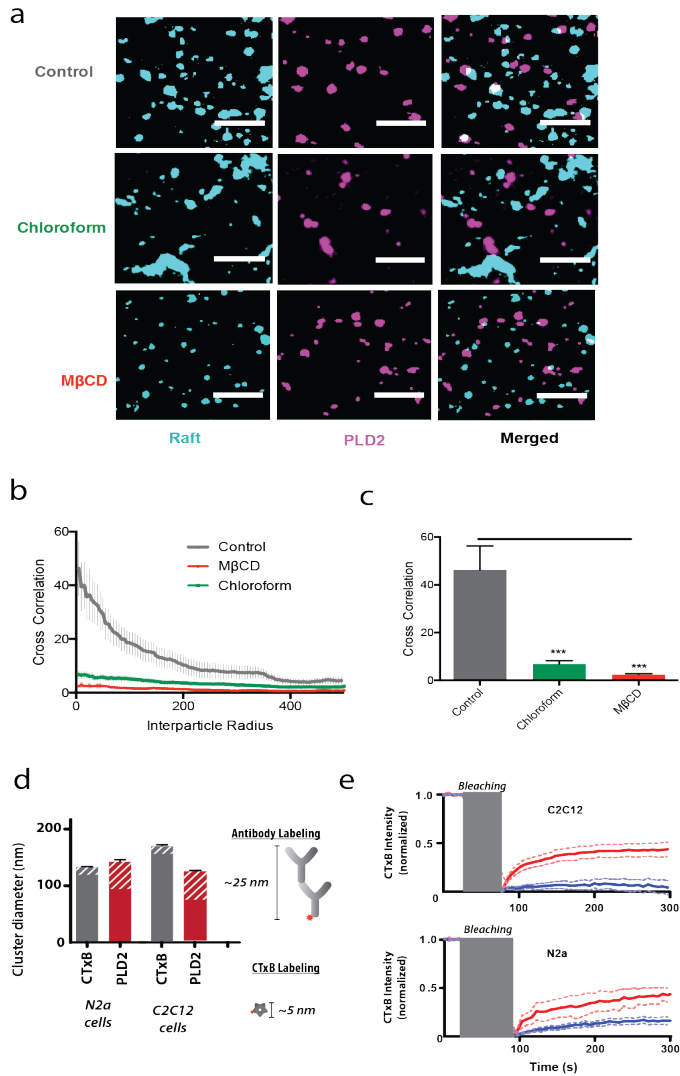


Fig. S5. Inhaled anesthetics displace PLD2 from GM1 rafts in C2C12 cells. **a**, Representative super-resolution (dSTORM) images of fluorescently labeled lipid raft (CTxB) and PLD2 before and after the treatment with chloroform (1 mM), and MβCD (100 μM) in C2C12 cells (Scale bars: 0.5 μm). **b-c**, Average Cross-correlation functions ($C(r)$) (**b**) and the function normalized at $C(r=5)$ (**c**) shows chloroform (1 mM) and MβCD (100 μM), disrupt PLD2 localization into lipid raft in C2C12 cells (\pm s.e.m., $n = 5$). **d**, Comparison of the cluster sizes (apparent raft sizes) of CTxB labeled GM1 rafts with the PLD2 antibody labeled proteins. Fixed PLD2 proteins have the same cluster size as CTxB labeled GM1 rafts suggesting CTxB may not cluster lipids after fixation treatment. The potential added diameter from CTxB or PLD2 labeling is indicated by white stripes. **e**, Movement of CTxB labeled lipids in N2A and C2C12 after fixation measured by Fluorescence recovery after photobleaching (FRAP). Student's t-test results: * $P < 0.05$; *** $P < 0.001$; **** $P < 0.0001$; NS $\geq P.0.05$.

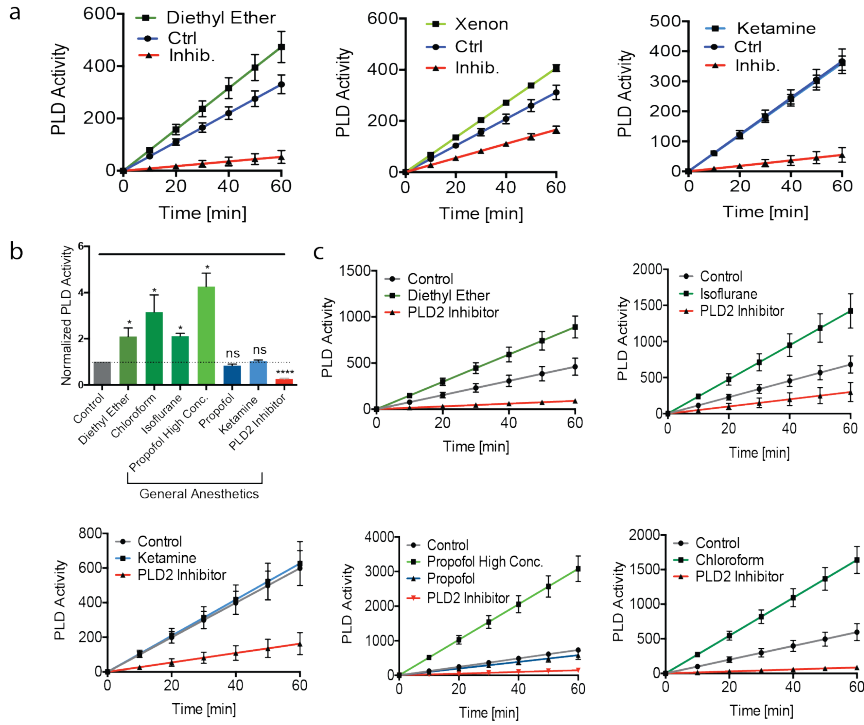


Fig. S6. Activation of PLD by inhaled anesthetics in N2A and C2C12 cells. **a**, PLD activity in N2A cells over 60 min when treated with diethyl ether (1 mM), xenon (4.9 mM) and ketamine (50 μ M). Diethyl ether and xenon have increased activity, but ketamine had no effect on PLD activity. PLD2 inhibitor (2.5-5 μ M) inhibited the activity (\pm s.e.m., $n = 4$). **b**, Normalized PLD activity in C2C12 cells after the 60 min anesthetic treatments as shown in (c). Diethyl ether (1 mM), chloroform (1 mM), isoflurane (1 mM), and higher concentration of propofol (400 μ M), but not 50 μ M propofol (green lines) activate PLD compared to control cells. Ketamine (50 μ M, blue line) had no observed effect on PLD activity. PLD inhibitor (2.5-5 μ M) inhibited the activity (\pm s.e.m., $n = 4$).